Astronomy
&
Astrophysics

Galaxy pairs align with Galactic filaments

E. Tempel and A. Tamm

Tartu Observatory, Observatooriumi 1, 61602 Tõravere, Estonia
e-mail: elmo.tempel@to.ee

ABSTRACT

Context. Gravitational collapse theory and numerical simulations suggest that the velocity field within large-scale galaxy filaments is dominated by motions along the filaments.
Aims. Our aim is to check whether observational data reveal any preferred orientation of galaxy pairs with respect to the underlying filaments as a result of the expectedly anisotropic velocity field.
Methods. We use galaxy pairs and galaxy filaments identified from Sloan Digital Sky Survey data. For filament extraction, we use the Bisous model that is based on the marked point process technique. During the filament detection, we use the centre point of each pair instead of the positions of galaxies to avoid a built-in influence of pair orientation on the filament construction. For pairs lying within filaments (3012 cases), we calculate the angle between the line connecting the galaxies of each pair and their host filaments. To avoid redshift-space distortions, the angle is measured in the plane of the sky.
Results. The alignment analysis shows that the orientation of galaxy pairs correlates strongly with their host filaments. The alignment signal is stronger for loose pairs, with at least 25% excess of aligned pairs compared to a random distribution. The alignment of galaxy pairs and filaments measured from the observational data is in good agreement with the alignment in the Millennium simulation and thus provides support to the ΛCDM formalism.

Key words. large-scale structure of Universe – galaxies: general – galaxies: interactions – galaxies: statistics

1. Introduction

The main driving force of structure formation in the expanding Universe is gravitational collapse. The collapse amplifies any initial anisotropy of matter distribution. As first pointed out by Zel'dovich (1970), the contraction is locally dominated by one dimension at a time. The speed of the collapse depends on the local density and the initial amplitude of perturbations, thus in numerical simulations, a complex pattern of nearly 2D sheets, nearly 1D filaments, and roughly spherical small density peaks (knots) develops, framing large under-dense void regions (Doroshkevich et al. 1980; Klypin & Shandarin 1983; Davis et al. 1985; Gramann 1993; Sheth & van de Weygaert 2004, etc.). Within this network, matter flows along well-defined paths, with the voids feeding the sheets, the sheets feeding the filaments, and the filaments finally channeling everything towards the knots (Cautun et al. 2014, and references therein).

Observational confirmation for the existence of a characteristic pattern of large-scale inhomogeneities was obtained decades ago (Jõeveer & Einasto 1978; Jõeveer et al. 1978; Peebles 1980; de Lapparent et al. 1986; Bond et al. 1996, etc.). However, the low number density of sufficiently luminous galaxies sets severe limits to the possibility of comparing the actual structures to the simulated ones. As a result, the fine structure and the dynamics of the actual cosmic web can be directly probed only within our local volume, which may not be representative of the Universe at larger scales. Nevertheless, the existing pieces of evidence regarding the dynamics within our super-Galactic neighbourhood support the void-sheet-filament-cluster sequence of matter flows (Tully et al. 2014; Tempel 2014; Karachentsev et al. 2014).

As an alternative to the simple mapping of structures, a method for testing and constraining structure formation

scenarios is provided by the alignment of structures. Anisotropic collapse and tidal torques should induce spinning up and stretching out of dark matter haloes along the general velocity field within a large-scale structure element (Codis et al. 2012; Aragon-Calvo & Yang 2014; Libeskind et al. 2014; Welker et al. 2014). Observationally, corresponding hints for some alignment between various structures have been found: elliptical galaxies and satellite systems around massive galaxies tend to be elongated in the direction of Galactic filaments (Tempel et al. 2013; Lee & Choi 2015; Zhang et al. 2015), while galaxy discs tend to be oriented perpendicular to filaments (Tempel et al. 2013; Tempel & Libeskind 2013). The former findings can be explained as a result of galaxy mergers and satellite accretion occurring along the filaments, while the latter effect can be reconciled with matter infall from voids and sheets around the filaments (Dubois et al. 2014).

In this paper we take a new step in alignment probing by measuring the angle between the orientation of galaxy pairs and the orientation of their host filaments. The pairs and filaments have been extracted from the Sloan Digital Sky Survey (SDSS). For filament detection we use the Bisous model, which is based on a marked point process (Tempel et al. 2014a). The Bisous filaments have already proven to be useful for probing the galaxy content and other properties of the cosmic web (e.g. Tempel et al. 2014b,c; Guo et al. 2015).

Throughout the paper we assume the *Wilkinson* Microwave Anisotropy Probe (WMAP) cosmology: the Hubble constant $H_0 = 100\,h$ km s^{-1} Mpc^{-1}, with $h = 0.697$, the matter density $\Omega_m = 0.27$, and the dark energy density $\Omega_\Lambda = 0.73$ (Komatsu et al. 2011).
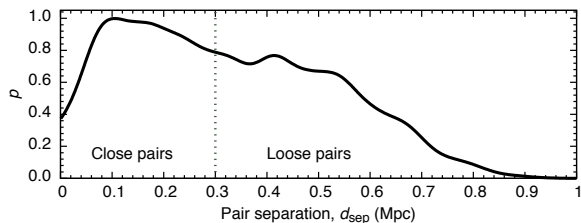
Fig. 1. Distribution of pair separations in the plane of the sky. The vertical dashed line splits the sample into two equal subsamples.

2. Data and methods

2.1. SDSS galaxy and group samples

This work is based on the SDSS data release 10 (York et al. 2000; Ahn et al. 2014). We use the galaxy and group samples as compiled in Tempel et al. (2014d), which cover the main contiguous area of the survey (the Legacy Survey). Galaxy groups are extracted using the conventional friend-of-friend (FoF) grouping algorithm with a varying linking length (see Tempel et al. 2014d, for more details). The flux-limited catalogue (apparent r-band magnitude limit is 17.77) extends to the redshift 0.2 (820 Mpc) and includes 588 193 galaxies and 82 458 groups with two or more members.

In Tempel et al. (2014d) the redshift-space distortions of galaxy groups are suppressed using the rms sizes of groups in the plane of the sky and their rms radial velocities as described in Liivamägi et al. (2012). Galaxies in groups are ascribed new radial distances in order to make the spatial distribution of galaxy groups approximately spherical. This compression removes the artificial line-of-sight filament-like structures and was necessary in order to retrieve a realistic filamentary pattern in the cosmic web.

For our analysis we use only galaxy pairs (galaxy groups with two members in the Tempel et al. 2014d catalogue) that are located within filaments (see Sect. 2.3 for the filament catalogue description). We consider a galaxy pair to be located in a filament if the geometrical centre point of the pair is closer than 0.5 Mpc to the filament axis. In total, this limits our sample to 3012 pairs. To avoid redshift-space effects, the separation between the galaxies in a galaxy pair is measured in the plane of the sky. The distribution of pair separations for pairs located in filaments is shown in Fig. 1.

Because of fibre collision in SDSS, some of the pairs in our sample are actually groups with three or more members. According to Tempel et al. (2012) the fraction of pairs that are affected by fibre collision is about 5%; hence, we can ignore this effect in the current analysis.

2.2. Semi-analytic galaxies in simulation

For a quick interpretation of the results, we use the distribution of galaxies in the Millennium simulation (Springel et al. 2005), in which dark matter haloes are populated with galaxies according to a semi-analytical galaxy formation model GAL-FORM (Bower et al. 2006). The simulated galaxy data and the Galactic filaments are the same as used in Guo et al. (2015) and Tempel et al. (2015) – see these papers for a more detailed description. For the analysis, we have only considered galaxies brighter than $M_r = -19$. The galaxy pairs (groups with two members) were extracted using the FoF algorithm with a linking length 0.5 h^{-1} Mpc. The pairs are separated into equal-sized close and loose pair samples according to the real separation

between galaxies. The limiting distance is 0.2 h^{-1} Mpc (i.e. roughly the same as for SDSS).

2.3. Galaxy filament sample for the SDSS data

The detection of filaments is performed by applying an object (marked) point process with interactions (the Bisous process; Stoica et al. 2005) to the spatial distribution of galaxies. This algorithm provides a quantitative classification that complies with the visual impression of the cosmic web and is based on a robust and well-defined mathematical scheme. More detailed descriptions of the Bisous model can be found in Stoica et al. (2007, 2010) and Tempel et al. (2014a). For convenience, a brief and intuitive summary is provided below.

Our model approximates the filamentary web with a random configuration of small segments. We assume that locally, galaxy conglomerations can be probed with relatively small cylinders that can be combined to trace a filament if the neighbouring cylinders are oriented similarly. An advantage of the approach is that it relies directly on the positions of galaxies and does not require any additional smoothing to create a continuous density field.

The solution provided by our model is stochastic. Therefore, we find some variation in the detected patterns for different Markov chain Monte Carlo (MCMC) runs of the model. On the other hand, thanks to the stochastic nature of the method we gain a morphological and statistical characterisation of the filamentary pattern simultaneously.

In practice, after fixing an approximate scale of the filaments, the algorithm returns the filament detection probability field together with the filament orientation field. Based on these data, filament spines are extracted and a filament catalogue is built in which every filament is represented by its spine as a set of points that defines the axis of the filament.

Our spine detection follows two ideas. First, filament spines are located at the highest density regions outlined by the filament probability maps. Second, in these regions of high probability for the filamentary network, the spines are oriented along the orientation field of the filamentary network. See Tempel et al. (2014a) for more details of the procedure.

For the current study, we have rebuilt the filament catalogue in order to eliminate the potential influence of galaxy pairs to the filament orientation. For filament extraction, each galaxy pair is replaced with a single point (the centre point of the two galaxies in the 3D space). In this way the orientation of a galaxy pair cannot affect the filament detection, and the orientations of filaments and galaxy pairs are measured independently.

The method and parameters for filament extraction are exactly the same as in Tempel et al. (2014a). The assumed scale (radius) of the filaments is roughly 0.7 Mpc[1]. Because the survey is flux-limited, the sample is very diluted farther away, and so we are able to detect filaments of this scale only up to the redshift 0.15 ($\approx$640 Mpc). To reduce the survey edge effects, we use only filaments that are farther than 10 Mpc from the survey boundary. In addition, to restrict ourselves to reliable filaments we dismiss all filaments shorter than 10 Mpc.

2.4. Measuring the alignment signal

As explained above, the determination of the orientation of filaments and the orientation of galaxy pairs are independent by construction and we do not have to worry about an intrinsic

---

[1] Most of the galaxies are close to the filament axis and 90% of galaxies inside 0.7 Mpc are closer than 0.5 Mpc to the filament axis.
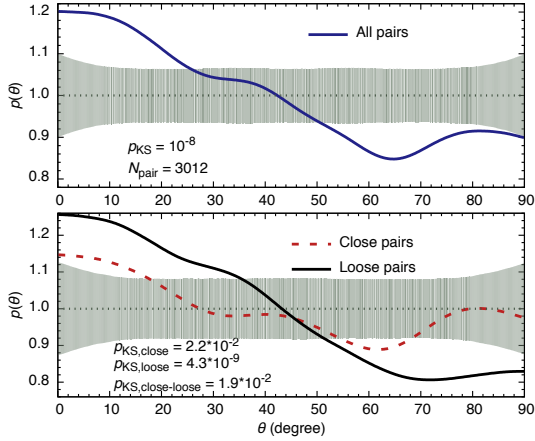
Fig. 2. *Upper panel*: probability distribution function (blue solid line) of the projected angles (in the plane of the sky) between galaxy pairs and their host filaments. The KS test probability that the sample is drawn from a uniform distribution is 10^{-8}. The filled area shows the 95% confidence region for a randomised distribution of 3012 pairs. *Lower panel*: same as in the upper panel for two equal-sized subsamples: close pairs ($d_{sep} < 0.3$ Mpc; red dashed line) and loose pairs ($d_{sep} > 0.3$ Mpc; black solid line).

Fig. 3. Distribution of stacked galaxy pairs in the plane of the sky. Galaxy pairs are stacked based on the orientation of the host filaments (represented by the x-axis); the centre point of each pair matches with the origin of the coordinate axes. The densities are shown in units of spherically averaged mean number densities. The black solid line shows the demarcation of close and loose pairs.
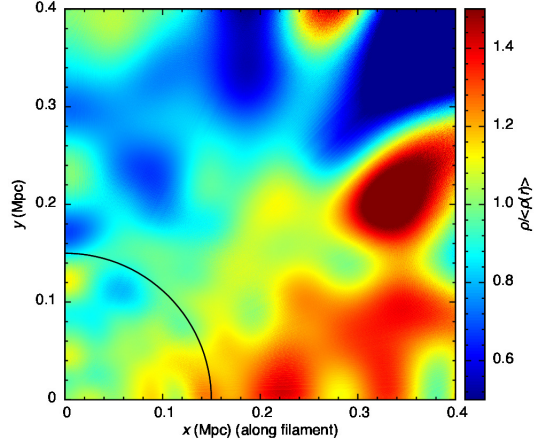
alignment caused by the method. However, the orientation of galaxy pairs and filaments is affected by the redshift-space distortions. To avoid any systematic effects introduced by the redshift-based distances, we measure the alignment in the plane of the sky. To this end we project galaxy pairs and filaments to the plane of the sky and measure the angle between filament orientation and pair orientation. The measured angle is restricted to the range of 0 to 90 deg. We calculate the alignment signal using a kernel density estimation[2].

To estimate confidence regions of the measured alignment signal, we generate 10 000 Monte Carlo samples with the same number of pairs as in the original sample and conduct the same alignment analysis. In the figures below, we show the 95% confidence regions for this randomised signal. The Kolmogorov-Smirnov test (KS test) probabilities that the angle distributions are drawn from a uniform distribution are also shown. To compare the two measured alignments, we use the KS test to calculate the probability that the distributions are drawn from the same distribution. The KS test values are indicated in the figures.

3. Results

Figure 2 (upper panel) shows the probability distribution of the angles between galaxy pair orientations and their host filament orientations. As explained above, the angles are measured in the plane of the sky in order to avoid possible effects of redshift-space distortions. It is seen that galaxy pairs are strongly aligned with Galactic filaments: the number of galaxy pairs aligned with the filament spine within ±10 deg is about 20% higher than it would be in the case of a random distribution, and the pair number decreases nearly monotonically when moving towards perpendicularity with the filament spine. The KS test probability that the alignment angles are drawn from a uniform distribution is $p_{KS} = 10^{-8}$ (~6.5σ signal).

In the lower panel of Fig. 2 we have split the pair sample into two equal-sized subsamples according to the projected distance between the galaxies of each pair. The demarcation between

close and loose pairs (0.3 Mpc) is indicated in Fig. 1. Figure 2 shows that galaxy pair alignment with Galactic filaments is much stronger for loose pairs than for close pairs, while the alignment significance remains above 95% (2σ) in both cases. The KS test probability that the close and loose pair samples are drawn from the same underlying distribution is 0.019, hence, the close and loose samples should be intrinsically different. However, the close-pair sample is contaminated by loose pairs oriented close to the line of sight, increasing the measured amount of non-aligned pairs.

We have also checked for the effect of sample splitting on the basis of various other measurable quantities: galaxy luminosity, colour, magnitude difference, distance, morphology, distance from filament axis, etc. In some cases, a small impact on the alignment signal was noticeable, but statistically insignificant. In principle, the statistical significance for the alignment signal can be increased either by increasing the sample size or by measuring the alignment in real space rather than in projection. The latter requires a proper treatment of redshift-space distortions, which is not a straightforward procedure and is beyond the scope of the present analysis.

To visualise the galaxy pair alignment in filaments, we show a stacked distribution of the galaxy pairs in the plane of the sky in Fig. 3. For the stacking, the centre point of pairs was fixed at the origin of the coordinate axes and all filaments were oriented along the x-axis. The figure shows that for the loose pairs, the alignment occurs uniformly across the whole range of separations. We note that the apparent density maximum in this figure around [$x = 0.35, y = 0.2$] is actually statistically insignificant – it corresponds to an enhancement of the random distribution by just a few galaxies at the given projected distance.

While the detected 2D alignment indicates that a significant fraction of galaxy pairs also has to be aligned with filaments in 3D space, a quantification and a more detailed interpretation of the measured signal is not straightforward owing to projection effects and redshift distortions. Instead, we can check whether the measured signal corresponds to the predictions of the ΛCDM formalism. To this end, using data from the Millennium simulation (as described above), we have studied the pair alignment with host filaments in the real space, splitting the pair sample into close and loose pairs according to the real-space

---

[2] In Appendix A of Tempel et al. (2014b) we show that the kernel density estimation is better than a simple histogram and is more representative of the underlying probability distribution.
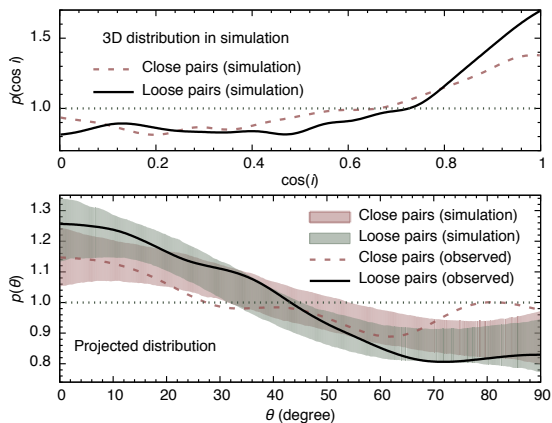
Fig. 4. *Upper panel*: alignment of close and loose galaxy pairs with the host filaments in the Millennium simulation; *i* denotes the real-space angle between a filament and a galaxy pair. *Lower panel*: angle distribution for close and loose pairs in the SDSS data (solid and dashed lines; same as in Fig. 2) compared to the sky projection of a model distribution, in which the real-space alignment between pairs and filaments of the Millennium simulation (shown in the upper panel) is ascribed to the actual SDSS filaments. The modelled distributions are shown as filled regions corresponding to the 95% confidence level.

distance[3]. The upper panel of Fig. 4 shows the resultant real-space alignment with the filaments in the simulation data. As in the case of the SDSS data, both subsamples show significant alignment, with close pairs being somewhat less aligned than the loose pairs. For a more direct comparison with the SDSS pairs, we have applied the alignment of the Millennium pairs to the SDSS filaments. In 2D projection, the resultant angle distribution is shown in the lower panel of Fig. 4 as filled regions. For loose pairs, the pair alignment of the simulation matches well with the observed one. For close pairs, the distributions nearly match within the 95% confidence level, except for angles beyond about 70 degrees, where the observed pairs seem to exhibit a population perpendicular to the host filaments. However, the mismatch can be a result of the sample variance and does not provide grounds for invalidating the simulation.

4. Conclusions and implications

We used the SDSS Legacy survey to analyse the alignment between Galactic filaments and galaxy pairs. The filamentary pattern in galaxy distribution was detected using the Bisous model and a catalogue of Galactic filaments was constructed. To overcome possible contamination by galaxy pair orientations, the galaxy pairs were treated as single points during the filament extraction. The alignment is measured in the plane of the sky to avoid redshift-space distortions.

The data show a clear tendency of galaxy pairs to align with their host filaments. The alignment is stronger for loose pairs and weaker for close pairs. The detected alignment is statistically highly significant, reaching up to 6.5σ. Quantitatively, the alignment is similar to the alignment measured for galaxy pairs and filaments extracted from the Millennium simulation, and are thus in concordance with the ΛCDM paradigm. Similar alignment is also present in a recent analysis of Local Group like pairs in a ΛCDM simulation (Forero-Romero & González 2015).

---
[3] The use of real-space distances guarantees that the dependence on pair separation is intrinsic and not affected by projection effects. However, when splitting the sample based on the projected distance, the measured alignment signals remain roughly the same.

Recently, the alignment of satellite galaxies and the cosmic web structures have been analysed by Lee & Choi (2015) and Tempel et al. (2015). Both studies conclude that the distribution of satellites around primary galaxies is elongated in the direction of Galactic filaments.

A simulation-based test carried out by Tempel et al. (2014c) showed that the given filament detection method also recovers the underlying velocity field. We can thus deduce that the alignment of galaxy pairs and satellite systems with their host filaments is a direct result of the anisotropic velocity field, leading towards a preferred direction of satellite accretion and gravitational collapse.

References

Ahn, C. P., Alexandroff, R., Allende Prieto, C., et al. 2014, ApJS, 211, 17
Aragon-Calvo, M. A., & Yang, L. F. 2014, MNRAS, 440, L46
Bond, J. R., Kofman, L., & Pogosyan, D. 1996, Nature, 380, 603
Bower, R. G., Benson, A. J., Malbon, R., et al. 2006, MNRAS, 370, 645
Cautun, M., van de Weygaert, R., Jones, B. J. T., & Frenk, C. S. 2014, MNRAS, 441, 2923
Codis, S., Pichon, C., Devriendt, J., et al. 2012, MNRAS, 427, 3320
Davis, M., Efstathiou, G., Frenk, C. S., & White, S. D. M. 1985, ApJ, 292, 371
de Lapparent, V., Geller, M. J., & Huchra, J. P. 1986, ApJ, 302, L1
Doroshkevich, A. G., Kotok, E. V., Poliudov, A. N., et al. 1980, MNRAS, 192, 321
Dubois, Y., Pichon, C., Welker, C., et al. 2014, MNRAS, 444, 1453
Forero-Romero, J. E., & González, R. 2015, ApJ, 799, 45
Gramann, M. 1993, ApJ, 405, 449
Guo, Q., Tempel, E., & Libeskind, N. I. 2015, ApJ, 800, 112
Jõeveer, M., & Einasto, J. 1978, in Large Scale Structures in the Universe, eds. M. S. Longair, & J. Einasto, IAU Symp., 79, 241
Jõeveer, M., Einasto, J., & Tago, E. 1978, MNRAS, 185, 357
Karachentsev, I. D., Karachentseva, V. E., & Nasonova, O. G. 2014, Astrophys., 57, 457
Klypin, A. A., & Shandarin, S. F. 1983, MNRAS, 204, 891
Komatsu, E., Smith, K. M., Dunkley, J., et al. 2011, ApJS, 192, 18
Lee, J., & Choi, Y.-Y. 2015, ApJ, 799, 212
Libeskind, N. I., Knebe, A., Hoffman, Y., & Gottlöber, S. 2014, MNRAS, 443, 1274
Liivamägi, L. J., Tempel, E., & Saar, E. 2012, A&A, 539, A80
Peebles, P. J. E. 1980, The large-scale structure of the universe (Princeton University Press)
Sheth, R. K., & van de Weygaert, R. 2004, MNRAS, 350, 517
Springel, V., White, S. D. M., Jenkins, A., et al. 2005, Nature, 435, 629
Stoica, R. S., Gregori, P., & Mateu, J. 2005, Stochastic Processes and their Applications, 115, 1860
Stoica, R. S., Martínez, V. J., & Saar, E. 2007, J. Roy. Statist. Soc. Ser. C, 56, 459
Stoica, R. S., Martínez, V. J., & Saar, E. 2010, A&A, 510, A38
Tempel, E. 2014, Nature, 513, 41
Tempel, E., & Libeskind, N. I. 2013, ApJ, 775, L42
Tempel, E., Tago, E., & Liivamägi, L. J. 2012, A&A, 540, A106
Tempel, E., Stoica, R. S., & Saar, E. 2013, MNRAS, 428, 1827
Tempel, E., Stoica, R. S., Martínez, V. J., et al. 2014a, MNRAS, 438, 3465
Tempel, E., Kipper, R., Saar, E., et al. 2014b, A&A, 572, A8
Tempel, E., Libeskind, N. I., Hoffman, Y., Liivamägi, L. J., & Tamm, A. 2014c, MNRAS, 437, L11
Tempel, E., Tamm, A., Gramann, M., et al. 2014d, A&A, 566, A1
Tempel, E., Guo, Q., Kipper, R., & Libeskind, N. I. 2015, MNRAS, submitted [arXiv:1502.02046]
Tully, R. B., Courtois, H., Hoffman, Y., & Pomarède, D. 2014, Nature, 513, 71
Welker, C., Devriendt, J., Dubois, Y., Pichon, C., & Peirani, S. 2014, MNRAS, 445, L46
York, D. G., Adelman, J., Anderson, Jr., J. E., et al. 2000, AJ, 120, 1579
Zel'dovich, Y. B. 1970, A&A, 5, 84
Zhang, Y., Yang, X., Wang, H., et al. 2015, ApJ, 798, 17